ARTICLE   OPEN

Check for updates

Proximity to a critical point driven by electronic entropy in URu$_2$Si$_2$

Neil Harrison [1]✉, Satya K. Kushwaha[1,2], Mun K. Chan [1] and Marcelo Jaime [1]

The strongly correlated actinide metal URu$_2$Si$_2$ exhibits a mean field-like second order phase transition at $T_o \approx 17$ K, yet lacks definitive signatures of a broken symmetry. Meanwhile, various experiments have also shown the electronic energy gap to closely resemble that resulting from hybridization between conduction electron and 5f-electron states. We argue here, using thermodynamic measurements, that the above seemingly incompatible observations can be jointly understood by way of proximity to an entropy-driven critical point, in which the latent heat of a valence-type electronic instability is quenched by thermal excitations across a gap, driving the transition second order. Salient features of such a transition include a robust gap spanning highly degenerate features in the electronic density of states, that is weakly (if at all) suppressed by temperature on approaching T_o, and an elliptical phase boundary in magnetic field and temperature that is Pauli paramagnetically limited at its critical magnetic field.

INTRODUCTION

URu$_2$Si$_2$ remains of immense interest owing to the possibility of it exhibiting a form of order distinct from that observed in other known materials[1]. The term "hidden order" (HO) has been coined[2,3] to describe the finding of an apparent Bardeen–Cooper–Schrieffer (BCS)-like phase transition at $T_o \approx$ 17 K[4,5], yet the absence of any definitive signatures of symmetry-breaking reconcilable with the entropy at the transition temperature[1]. Whereas the majority of the proposed forms of HO[3,6–22] involve translational symmetry breaking[3,8–22], the experimental evidence in favor of this is indirect (see Methods)[23–28]. By contrast, neutron scattering, x-ray scattering, and scanning tunneling microscopy studies of URu$_2$Si$_2$ have shown that the usual momentum-space signatures of translational symmetry-breaking are missing within the HO phase[29–31]. The form of the electronic energy gap within the HO phase is found instead to be consistent with the opening of a hybridization gap between conduction and f-electron states centered on the chemical potential μ, as shown schematically in Fig. 1[29–33]. This gap has further been reported to evolve into a pseudogap at temperatures above T_o[32,34,35], suggesting departures from the Landau formalism.

The motivation for the present study is the realization that a HO phase corresponding to the formation (or opening) of a hybridization gap centered on μ would be expected to exhibit thermodynamic signatures distinct from those of a BCS-like phase transition[36–39]. For example, since the process of hybridization causes f electrons to become more delocalized (see Fig. 1)[40,41], such a phase transition would be expected to be accompanied by changes in the 5f-electron core occupancy and valence[42], thereby displaying some parallels to valence transition systems. Furthermore, since all of the available states in a narrow f-electron band (i.e., two electrons per formula unit—one filled and one empty) typically participate in the formation of hybridization gap[40,41], in contrast to the small fraction of the carriers in a conduction band that participate in the formation of a BCS-like gap[36–39], significant differences in the entropy of the quasiparticle excitations would be expected in thermodynamic experiments. Finally, since there is

no absolute requirement for the magnitude of a hybridization gap to vanish at a phase transition, it need not be thermally suppressed in the same manner as a BCS-type gap.

Experimental observations that could already be considered conducive to 5f-electron hybridization playing an important role in URu$_2$Si$_2$ include the intermediate valence character of the 5f electrons identified in x-ray scattering studies[43,44] and the finding of measureable volume and lattice changes across the HO transition in dilatometry experiments[45,46], which become increasingly sharp under a strong magnetic field[47,48].

We show here by way of thermodynamic[49,50] measurements that the HO phase in URu$_2$Si$_2$ exhibits signatures consistent with a critical point. In this unprecedented case, a discontinuous electronic phase transition into a state with a robust hybridization gap between the conduction and f electrons centered on μ becomes concealed as a mean field-like second-order phase transition owing to the effect of substantial quasiparticle excitations across the gap. We find the gap excitations, which are responsible for the exponential tail in the low temperature ($T < T_o$) heat capacity[4,5], to contribute significantly more to the internal energy than they do to the free energy, leading to an unusual situation in which the transition manifests itself second order in nature in all the observables, while maintaining some characteristics of a discontinuous phase transition. These include a robust gap that is weakly (if at all) suppressed by temperature, spanning highly degenerate features in the electronic density of states that are quantitatively consistent with a half-filled narrow f-electron band that has become gapped[29,30] (see Fig. 1), and an elliptical phase boundary that is usually the hallmark of valence transition systems[51–53]. The effective g-factor characterizing the ratio of the Pauli-limited critical magnetic field B_o to the critical temperature T_o is in quantitative agreement with prior measurements[54–56]. The near-degeneracy in the free energies of the HO and paramagnetic phase over a range of temperatures $T \geq T_o$ further causes the hybridization gap in URu$_2$Si$_2$ to become highly susceptible to the formation of a pseudogap[34,35], should fluctuations or inhomogeneities be present.

[1]MPA-MAGLAB, Los Alamos National Laboratory, Los Alamos, NM, USA. [2]MPA-Q, Los Alamos National Laboratory, Los Alamos, NM, USA. ✉email: nharrison@lanl.gov
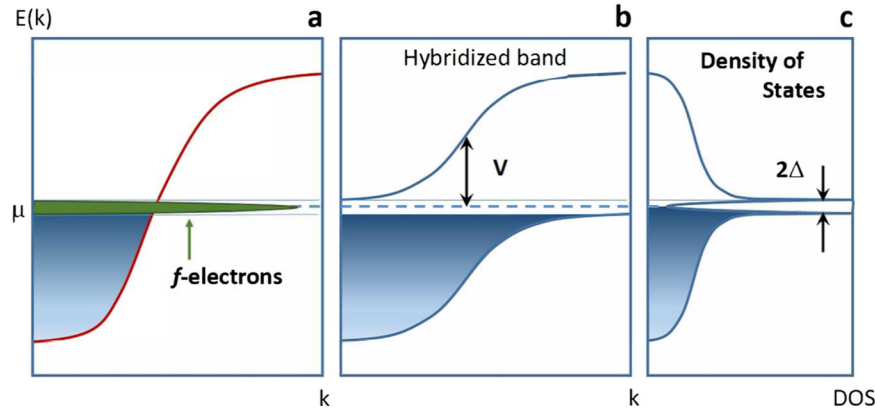
Fig. 1 Formation of a hybridization gap. a Conduction electron band (red) and weakly dispersive f-electron band (green) in the absence of a hybridization gap. **b** Hybridization bands forming at low temperatures, where V is the hybridization potential. **c** Indirect gap 2Δ separating peaks in the electronic density of states.

RESULTS

Thermally robust hybridization gap

The salient feature of the HO phase in URu_2Si_2 is a sharp anomaly in the specific heat suggestive of a continuous phase transition (see Fig. 2 and Methods)[1–5,49,57]. One of the more striking properties of this transition is an exponential tail that extends over a broad range of temperatures and is often compared to the exponential tail observed in BCS-type phases at low temperatures[36–39]. In the BCS theory[36], the excitation gap Δ causing the exponential tail has the form $C \propto e^{-\frac{\Delta}{T}}$, where $\Delta = aT_c$, $a \approx 1.5$, and T_c is the transition temperature. Were one to set $T_c = 17$ K, the BCS theory would predict an excitation gap of $\Delta \approx 25$ K for which the population of excited quasiparticles ($\sim e^{-\frac{\Delta}{T}}$) would reach at least $\approx 22\%$ of its saturated value as the transition temperature is approached from below. In such a scenario, the excitation of quasiparticles across the gap would cause a suppression of the amplitude of the order parameter with increasing temperature, and its ultimate closure at the phase transition temperature. This closure would, in turn, cause the number of quasiparticles excited across the gap to reach 100%. By contrast, previous reports of a much larger excitation gap of $\Delta \sim 100$ K in URu_2Si_2[4,5] imply that only a small population of excited quasiparticles of order ~0.3% occurs on reaching the transition temperature. This is too small a fraction for Δ to be significantly suppressed by thermal excitations in the manner of a BCS-type phase transition.

A further difficulty with the application of the BCS phenomenology to URu_2Si_2 is that its validity requires only a small fraction ($n_\Delta \ll 1$ electrons per formula unit) of the carriers in the conduction band to be displaced in energy on either side of the chemical potential when the gap opens[36–39]. However, when we estimate the number of electrons displaced by the opening of a 2Δ-wide BCS gap in URu_2Si_2 (using $\Delta = 100$ K), we obtain $n_\Delta = 2\Delta D(\varepsilon) = 6\Delta \times \Delta\gamma/\pi^2 R \sim 0.5$ electrons per formula unit (where R is the gas constant). We base this estimate on the entropy $S_{exp} = \Delta\gamma T_o$ associated with the formation of the HO phase having been found experimentally by the integration of C_{exp}/T to be $S_{exp} = 0.2\, R\ln 2$ (see Fig. 3)[4,5], for which the change in Sommerfeld coefficient at T_o is $\Delta\gamma \approx 68$ mJmol^{-1}K^{-2}. Since our estimate of $n_\Delta \sim 0.5$ electrons per formula unit corresponds to a significant fraction of a band, it implies that a major reconfiguration of the electronic bands accompanies the formation of the HO phase in URu_2Si_2.

In the case of a hybridization gap, by contrast, the majority of the gapped states originate from an f-electron band (or level) that is already likely to have been highly degenerate prior to the onset of a hybridization gap, as shown schematically in Fig. 1a. When hybridization occurs at a characteristic energy V between the conduction electron and a coherent lattice of f electrons (see Fig.
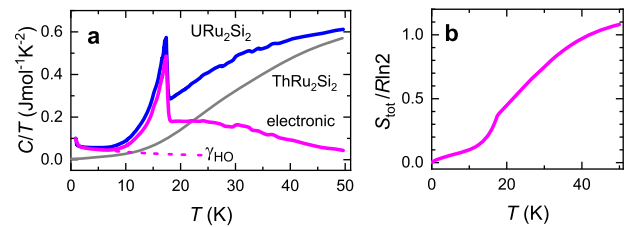

Fig. 2 Heat capacity and entropy of URu_2Si_2. a C/T at $B = 0$ from ref. [57] (blue line), with the phonon (i.e., $ThRu_2Si_2$ in gray) component and the total electronic contribution (magenta curve) indicated. γ_{HO} is the residual electronic contribution within the hidden-order phase (see Methods). **b** Total entropy obtained from $S_{tot} = \int_0^\infty (C_e/T)dT$, where C_e is the total electronic contribution to the heat capacity.
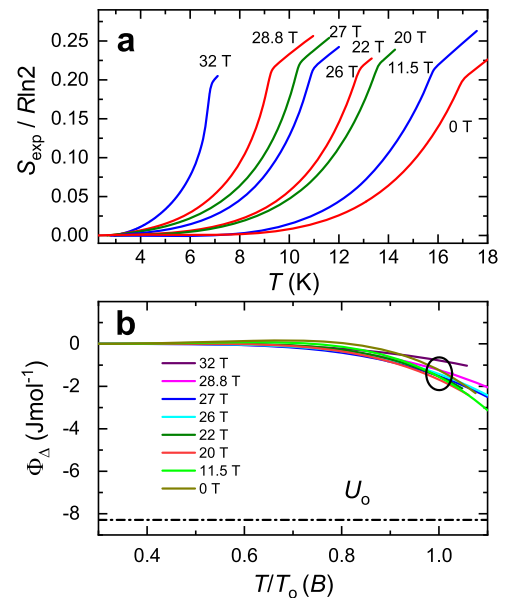

Fig. 3 Electronic entropy and free energy of quasiparticle excitations in URu_2Si_2. a The entropy divided by $R\ln 2$ (where $R = k_B N_A$) at different values of the magnetic field calculated using $S_{exp} = \int_0^\infty \frac{C_{exp}}{T}dT$ where C_{exp} refers to the measured heat capacity after subtracting the phonon contribution and γ_{HO} (see Methods). The entropy is similar to that previously obtained[4,5]. **b** Φ_Δ calculated from the experimental heat capacity data of URu_2Si_2 using Eq. (2) as described in the Methods at different magnetic fields as indicated. The horizontal axis is the temperature T divided by the observed transition temperature $T_o(B)$ at each magnetic field.

1b), the majority of the f-electron states become piled up at energies $\pm\Delta$ on either side of the gap (see Fig. 1c), where $\Delta \ll V$. In such a situation, 2Δ usually corresponds to the indirect gap shown schematically in Fig. 1b, c. On assuming the chemical potential to be located at $\mu = 0$, a more appropriate approximation for the gap is an electronic density of states of the form

$$g_\Delta(\varepsilon) = \frac{n_f}{2} \sum_{i=\pm 1} \delta(\varepsilon - i\Delta) \qquad (1)$$

consisting of delta functions, where each is comprised of $n_f/2 \approx 1$ electron per formula unit and is separated from the other by a gap 2Δ. The level below the chemical potential is filled, whereas that above the chemical potential is empty. We assume a Kondo semimetallic ground state in which a hybridization gap coexists with small ungapped sections of Fermi surface; the latter likely originate from a small finite dispersion of the unhybridized f-electrons and are responsible for the residual specific heat (γ_{HO} in the Methods) and quantum oscillations. Assuming a density of states of the form given by Eq. (1), the quasiparticle excitation term to the free energy of the HO phase is given by

$$\Phi_\Delta = -n_f RT \int_{-\infty}^{\infty} g_\Delta(\varepsilon) \ln\left(1 + e^{-\frac{\varepsilon}{T}}\right) d\varepsilon - \Phi_0 \\ = -n_f RT \ln\left(1 + e^{-\frac{\Delta}{T}}\right), \qquad (2)$$

where Φ_0 is a constant whose value enforces the constraint $\Phi_\Delta \to 0$ in the limit $T \to 0$. While we assume the gap to be symmetric with regard to μ, the same form for the free energy is obtained for the case of n_f electrons contained in a single delta function located at $\varepsilon = +\Delta$ or $\varepsilon = -\Delta$. On calculating the specific heat, we find the Schottky form

$$C_\Delta = -T \frac{\partial^2 \Phi_\Delta}{\partial T^2} = \frac{n_f R \Delta^2}{T^2} \frac{e^{-\frac{\Delta}{T}}}{\left(1 + e^{-\frac{\Delta}{T}}\right)^2}, \qquad (3)$$

where $e^{-\frac{\Delta}{T}} \ll 1$. We obtain $\Delta = 84 \pm 2$ K to reasonable accuracy by performing a straight line fit to an Arrhenius plot of the experimentally measured specific heat C_{exp} multiplied by T^2 (shown in Fig. 4). The finding of a straight line up to ~14 K suggests that Δ remains largely unchanged up to this temperature, which corresponds to $\approx 80\%$ of T_o.
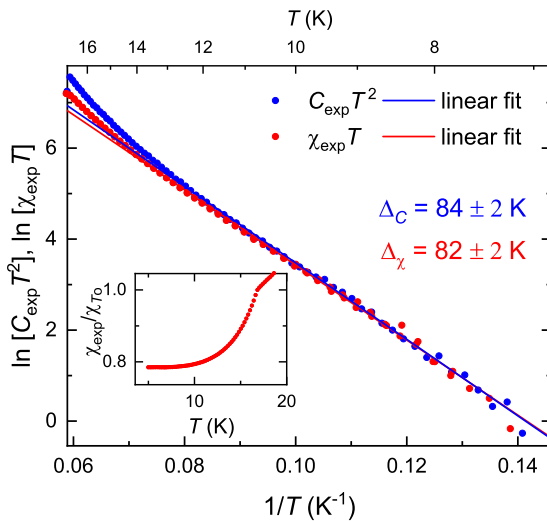

Fig. 4 Arrhenius plot. $\ln[C_{exp}T^2]$ (blue circles) versus $1/T$ at $B = 0$, which we fit to $\ln[C_\Delta T^2]$ (blue line) where C_Δ is given by Eq. (3). We compare this against $\ln[\chi_{exp}T]$ (red circles, shifted to bring it into alignment with the specific heat) fit to χ_Δ (red line) given by Eq. (4), where χ_{exp} is the measured susceptibility (shown in the inset). Solid lines fits are used to provide gap estimates Δ_C and Δ_χ, obtained from the specific heat and susceptibility, respectively.

An identically large hybridization gap governing the quasiparticle excitations is evidenced by the presence of a similar activated behavior in the susceptibility (also shown in Fig. 4). We model the spin susceptibility using

$$\chi_\Delta = \mu_0 [g_{eff}^* \sigma \mu_B]^2 R k_B^{-1} \int_{-\infty}^{\infty} f'_{FD}(\varepsilon) g(\varepsilon) d\varepsilon \\ = \frac{n_f \mu_0 [g_{eff}^* \sigma \mu_B]^2 R}{k_B T} \frac{e^{-\frac{\Delta}{T}}}{\left(1 + e^{-\frac{\Delta}{T}}\right)^2}, \qquad (4)$$

where $f'_{FD}(\varepsilon)$ is the energy derivative of the Fermi–Dirac distribution function. Figure 4 shows that the experimental C_{exp} and χ_{exp} data in URu$_2$Si$_2$ are characterized by similar values of the excitation gap Δ within experimental uncertainty, indicating that the spin and charge excitations are representative of the same electronic states. The observation of an activated behavior somewhat closer to T_o in the susceptibility reinforces the finding from heat capacity measurements of a large mostly temperature-independent gap. It also represents a marked departure from the case of a BCS-like order parameter, such as a charge-density wave[58], where the gap magnitude shrinks and rapidly fills in with thermally excited quasiparticles close to the transition.

The values of Δ in Fig. 4 are of comparable magnitude to those typically found in optical conductivity and tunneling experiments[29,30,32,33,59,60]. We find stronger quantitative consistency with the range of gap values, $63 \leq \Delta \leq 82$ K, attributed to hybridization in point contact spectroscopy experiments (see Fig. 3c, d of refs [32,33]), thereby reinforcing our interpretation that the exponential tail of the heat capacity anomaly in URu$_2$Si$_2$[1–5] is caused by quasiparticle excitations across a hybridization gap rather than a BCS-type gap.

Participation of two electrons per formula unit

The Arrhenius fit of Eq. (3) to the specific heat data also provides us with a means to extract an experimental estimate for the absolute number n_f of f-electron states participating in the hybridization gap. From the intercept $\ln[n_f R \Delta^2] \approx 11.9$ of the Arrhenius plot in Fig. 4, we obtain $n_f \approx 2.47 \pm 0.25$ per formula unit, which corresponds to roughly two $5f$ electrons per formula unit—again, suggesting one filled and one empty. This value is significantly larger than the estimate of $n_\Delta \approx 0.4$ electrons displaced by the gap that we obtain on substituting $\Delta = 84$ K into $n_\Delta = 2\Delta D(\varepsilon) = 6\Delta \times \Delta\gamma/\pi^2 R$, suggesting that the $n_f \approx 2$ electrons participating in the formation of the hybridization gap must involve states that are much farther from the Fermi surface than those typically participating in a BCS-type gap. This can include states that are farther removed from the chemical potential than $\pm\Delta$ or f electrons that are confined to the atomic core above T_o.

Entropy considerations add further weight to a scenario in which the number of electrons participating in the gap are too numerous to have originated from states close to the Fermi surface. Since the entropy of the gap excitations is given by

$$S_\Delta = -\frac{\partial\Phi_\Delta(B,T)}{\partial T} \\ = n_f R \left[\ln\left(1 + e^{-\frac{\Delta}{T}}\right) + \frac{\Delta}{T} \frac{e^{-\frac{\Delta}{T}}}{\left(1 + e^{-\frac{\Delta}{T}}\right)} \right], \qquad (5)$$

on substituting $n_f \approx 2$ electrons per formula unit participating in the gap we arrive at a total "projected" entropy (on taking the limit $\Delta \to 0$) of $S_\Delta \approx R \ln 4$. This is ten times larger than the experimentally observed entropy associated with the transition of $S_{exp} \approx 0.2 R \ln 2$ (see Fig. 3 and Methods)[4,5] at T_o, and twice as large as the total electronic entropy $S_{tot} \approx R \ln 2$ obtained on integrating the full electronic contribution to C/T (magenta curve in Fig. 2a) up to 50 K in Fig. 2b. One way to reconcile the existence of a gapped f-electron band supporting a projected electronic entropy of $R \ln 4$ (were this to persist beyond T_o) with an actual integrated total electronic entropy of $R \ln 2$ at $T = 50$ K ~ T_K is if T_o involves a transition from a screened Kondo lattice state consisting of local
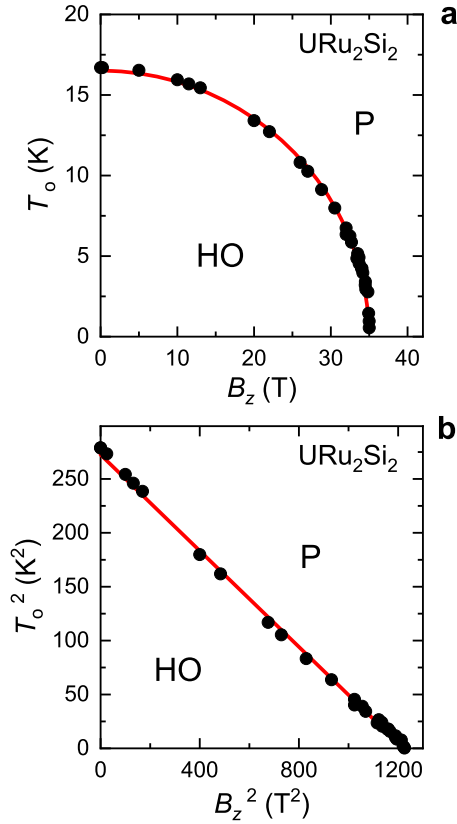
Fig. 5 Elliptical phase diagram. a $T_o(B_z)$ phase boundary of URu₂Si₂, taken from the peak in the specific heat capacity at the transition[49,50] and the step in the resistivity at high fields[74], where B_z refers to the magnetic field applied along the crystalline c-axis. The solid line represents a fit to Eq. (7). We neglect the additional phase transitions at $B \gtrsim 36$ T[74]. **b** Same data plotted in T_o^2-versus-B^2 coordinates.

spins with a twofold degeneracy at $T > T_o$ into a partially gapped state with fully itinerant f electrons including spin and charge degrees of freedom at $T < T_o$. A transition of this nature has indeed been suggested on the basis of scanning tunneling microscopy studies[29,30], which find a hybridization gap at $T < T_o$ and single impurity-type behavior at $T > T_o$[30].

Elliptical phase boundary

Further support for a robust hybridization gap and a significant change in the electronic structure accompanying the transition in URu₂Si₂ is to be found in the elliptical form of the phase boundary (see Fig. 5). This can be understood phenomenologically by considering a minimal model for the free energies of the paramagnetic (P) and the HO phases of the form

$$F'_P = -\tfrac{1}{2}\Delta\gamma T^2 - \tfrac{1}{2\mu_0}\Delta\chi_{zz}B_z^2$$
$$F'_{HO} = -U_o + \Phi_\Delta(B, T). \tag{6}$$

An important factor in determining our choice of F'_P in URu₂Si₂ is that the Kondo temperature $T_K \sim 70$ K[61,62] greatly exceeds T_o, suggesting the development of Kondo screening[40] well in advance of the transition at T_o. The Sommerfeld coefficient and spin susceptibility are both found to be strongly enhanced at temperatures both above and below T_o[4,5,63,64], while quantum oscillation experiments[54,65,66] find moderately enhanced quasiparticle effective masses deep inside the HO phase.

While Kondo screening implies that there is a finite V within the paramagnetic phase at $T > T_o$, there is a lack of thermodynamic evidence for a gap (see Fig. 2 and Methods for alternative

possibilities)—there is, however, spectroscopic evidence for a broadened gap possibly attributed to a pseudogap for a narrow range of temperatures above T_o[32,34,35] (see Methods). Given the comparatively slowly varying electronic contribution to C/T with temperature at $T > T_o$, as a simplifying measure, we consider constant changes $\Delta\gamma$ and $\Delta\chi_{zz}$ in the respective Sommerfeld coefficient and the c-axis spin susceptibility between the paramagnetic and HO phases in Eq. (6), and neglect terms that are common to both phases (such as that due to phonons). Also, since the spin susceptibility exhibits a strong Ising-like anisotropy[23,54,55,67,68] on both sides of the transition, $B_z = B\cos\theta$ refers here to the c-axis component of the magnetic field, while U_o represents the internal energy gained by the formation of the hybridization gap; we assume U_0 to be approximately constant in view of the robust Δ (see Methods). One advantage of adopting such a simple form for the free energy is that it can be compared directly against specific heat measurements without needing to assume a priori whether the Ehrenfest classification[69] of the transition is of first or second order, or the question of whether a symmetry is broken.

Since a phase transition is defined as the point at which $F'_P = F'_{HO}$, a value for U_o that remains finite and positive at the transition allows us to obtain an equation for the phase boundary that has the elliptical form

$$\left(\frac{T_o(B)}{T_o(B=0)}\right)^2 + \left(\frac{B_z}{B_o}\right)^2 = 1, \tag{7}$$

where

$$2[U_o - \Phi_\Delta(B, T)] = \Delta\gamma T_o^2 \equiv \mu_0^{-1}\Delta\chi_{zz}B_o^2. \tag{8}$$

This form is verified by the experimental finding of an elliptical form for the phase boundary for URu₂Si₂ in Fig. 5. A near constant U_o corresponds to the phase boundary having a similar form to that of valence transition systems[51–53]. Another important factor in the elliptical shape of the phase boundary is the finding that the excitation term $\Phi_\Delta(B, T)$ in Fig. 3b is a small contribution to the free energy for $T \leq T_o$, (see Methods) and rises to nearly the same value at the phase boundary for all values of the applied magnetic field.

Pauli paramagnetic limiting

Our findings that the spin and charge excitations in Fig. 4 are governed by the same gap (further supported by the reduction in carrier number found in Hall effect measurements)[61] and that the phase boundary is primarily determined by a simple balance between quadratic energy terms imply that the excitations behave as though they were conventional quasiparticles. We confirm this by showing that the HO phase boundary is Pauli paramagnetically limited. Turning to the phase boundary given by Eq. (7), we expect changes in the values of the Sommerfeld coefficient $\Delta\gamma = \frac{\pi^2}{3}k_B^2\Delta D(\varepsilon)$ and the spin susceptibility $\Delta\chi_{zz} = \mu_0[g^*_{eff}\sigma\mu_B]^2\Delta D(\varepsilon)$ to be defined in terms of the same change in the electronic density of states $\Delta D(\varepsilon)$[70]. The ratio $T_o/B_{o,\theta}$ of the transition temperature to the strength of the critical magnetic field therefore depends solely on the effective quasiparticle g-factor

$$g^*_{eff,\theta} = \frac{2\pi k_B}{\sqrt{3}\mu_B}\frac{T_o}{B_{o,\theta}} \tag{9}$$

(assuming $\sigma = \frac{1}{2}$ pseudospins). Here, $g^*_{eff,\theta} \approx g^*_{eff}\cos\theta$ refers to the angle-dependent effective g-factor (including its renormalization by Landau Fermi liquid parameters) that accounts for Zeeman splitting of the Landau-level states observed in quantum oscillation experiments[54] and the spin susceptibility of the Fermi liquid state that competes with superconductivity within the HO phase at low temperatures[55]. On inserting the previously measured[71] angle-dependent critical magnetic field $B_{o,\theta}$ of the HO phase into Eq. (9), we obtain excellent quantitative agreement
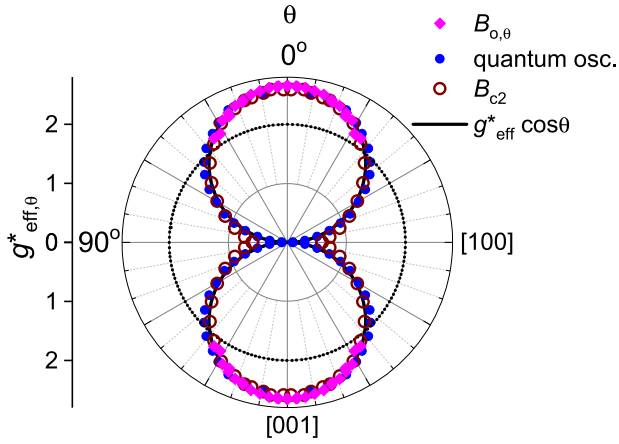
Fig. 6 Polar *g*-factor plot. Angle θ-dependent $g^*_{\text{eff},\theta}$ (magenta diamonds) obtained from θ-dependent critical magnetic field $B_{\text{o},\theta}$ of the hidden-order phase[71] using Eq. (9). This is compared against prior g-factor estimates from spin zeroes in the quantum oscillation amplitude[54] (blue filled circles) and the upper critical field B_{c2} of the Pauli-limited superconducting state[55] (open brown circles) within the hidden-order phase. The solid black line represents $g^*_{\text{eff}} = g^*_{\text{eff}} \cos \theta$, while the dotted line represents an isotropic $g = 2$.

between the angle-dependent $g_{\text{eff},\theta}$ and prior estimates of $g_{\text{eff},\theta}$ from quantum oscillation and Pauli-limited superconducting upper critical field measurements in Fig. 6[54,55]. These findings are, again, consistent with U_{o} and Δ both being largely robust against an increase in temperature within the HO phase.

Our finding that the critical field is determined by Eq. (9), and not the conventional expression[72,73]

$$g^*_{\text{eff},\theta} = \frac{\sqrt{2} k_B \Psi}{\mu_B B_{\text{P},\theta}} \tag{10}$$

for the Pauli paramagnetic limit defined in terms of an order parameter Ψ, is another strong indication that the HO gap in URu_2Si_2 is caused by hybridization rather than a conventional BCS-like order parameter. While Eq. (10) has been shown to be valid for the superconducting phase of URu_2Si_2[55], setting $\Psi = \Delta$ in Eq. (10) would yield a 90% overestimate for the critical field of the HO phase.

Quenched latent heat at the transition

The experimental observations presented thus far are suggestive of a discontinuous phase transition in URu_2Si_2. The gap is found to retain a large amplitude close to the phase transition (in Fig. 4), with the pre-factor of the specific heat indicating that $n_f \approx 2$ electrons participate in its formation. The phase boundary is further found to have the elliptical form (in Fig. 5) in common with first-order valence transitions systems, and a critical field that is Pauli paramagnetically limited (in Fig. 6). Experimentally, however, the transition is found to be of first order only near the upper critical field B_{o} of the HO phase[47–49,64,74].

A key feature of URu_2Si_2 that distinguishes it from established valence transition systems is the presence of quasiparticle excitations across a gap. Whereas these excitations give rise to a large contribution to the specific heat for $T < T_{\text{o}}$ (see Methods)[4,5], their contribution to the free energy is comparatively small—too small, in fact, to cause a significant departure of the phase boundary from an ideal elliptical form in Fig. 5. The entropic energy term $S_\Delta T$ is, however, found to be large enough to almost completely quench the latent heat at the transition. This can be demonstrated by comparing the relative free and internal energies of the paramagnetic and HO phases in Fig. 7. Figure 7a, b shows the relative free energies of the paramagnetic and HO
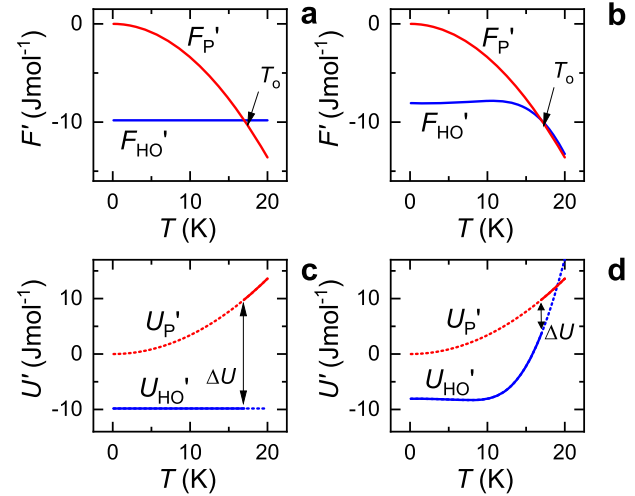

Fig. 7 Free and internal energies. a Free energies according to Eq. (6) in the absence of thermal excitations (i.e., $\Phi_\Delta = 0$) at $B = 0$ for the paramagnetic (P) and hidden-order (HO) phases, computed using $\Delta\gamma = 68 \text{ mJmol}^{-1}\text{K}^{-2}$ (parameter similar to that found in URu_2Si_2 at $B = 0$)[5] and $U_{\text{o}} \approx 10 \text{ Jmol}^{-1}$. At the transition T_{o}, $F'_{\text{P}} = F'_{\text{HO}}$. **b** Free energies according to Eq. (6) inclusive of thermal excitations, computed using $\Delta\gamma = 68 \text{ mJmol}^{-1}\text{K}^{-2}$, $\Delta = 84$ K, and $U_{\text{o}} \approx 8 \text{ Jmol}^{-1}$. **c** Internal energies according to Eq. (11) in the absence of thermal excitations (i.e., $\Phi_\Delta = 0$) at $B = 0$. **d** Internal energies according to Eq. (11) inclusive of thermal excitations. The latent heat at the transition is given by ΔU.

phases obtained using Eq. (6), both in the absence (by artificially setting $\Phi_\Delta = 0$ in Fig. 7a) and presence (by setting $\Delta = 84$ K in Φ_Δ in Fig. 7b) of quasiparticle excitations across the gap. The parameter U_{o} has been arbitrarily adjusted so that $\Delta F = F'_{\text{HO}} - F'_{\text{P}} = 0$ at the known transition temperature.

We proceed to extract the relative internal energies of the two phases in the absence (again, by artificially setting $\Phi_\Delta = 0$ in Fig. 7c) and presence (again, by setting $\Delta = 84$ K in Φ_Δ in Fig. 7d) of gap excitations. The relative internal energies are therefore given by

$$U'_{\text{P}} = \frac{1}{2}\Delta\gamma T^2 - \frac{1}{2\mu_0}\Delta\chi B^2$$
$$U'_{\text{HO}} = -U_{\text{o}} + \Phi_\Delta(B, T) + TS_\Delta, \tag{11}$$

where S_Δ is the entropy associated with gap excitations given by Eq. (5). Figure 7 shows that whereas the absence of gap excitations ordinarily leads to a large latent heat ΔU at the transition (see Fig. 7c), analogous to that encountered in valence transition systems[51–53], the presence of quasiparticle excitations in Fig. 7d causes ΔU to be quenched in the vicinity of the transition; we find that ΔU vanishes within ~3 K of the transition temperature in URu_2Si_2.

Change in the Ehrenfest classification of the transition

Depending on the degree of suppression of the latent heat, the Ehrenfest classification[69] of the transition therefore has the potential either to be of first or second order in URu_2Si_2. The order of the transition is ultimately determined by the form of the departure of the measured specific heat C_{exp} (blue circles in Fig. 4) near the transition temperature from the ideal Arrhenius form C_Δ (blue line in Fig. 4) given by Eq. (3). This places quantitative constraints on the manner in which the hybridization gap and phase transition evolve as a function of temperature. In Fig. 8, we extend the fits of C_Δ (black curves) to the measured specific heat C_{exp} (red, green, and blue curves) to different magnetic field values, showing the departure of C_Δ from C_{exp} to become larger with increasing magnetic field.
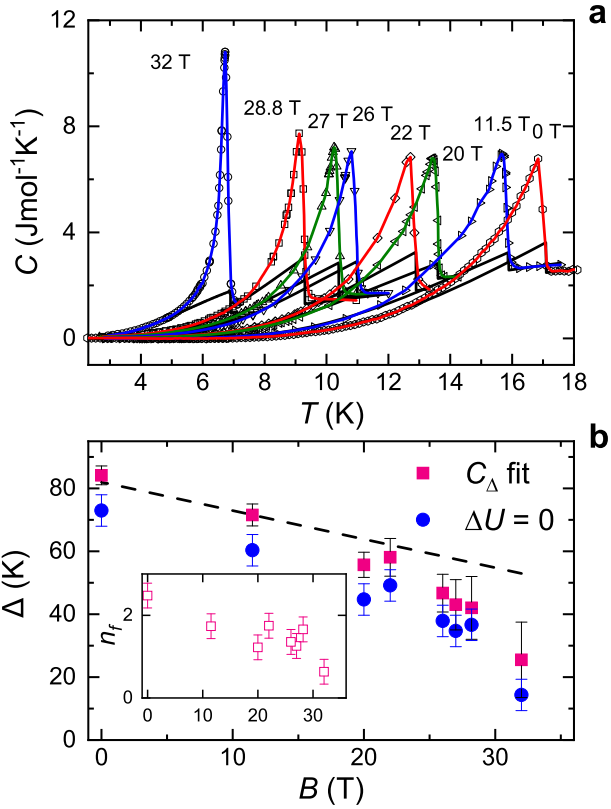
Fig. 8 Fits to the electronic specific heat. a The measured electronic specific heat $C_{exp}(T)$ of URu$_2$Si$_2$ (data points from ref. [49], after having subtracted γ_{HO}; see Methods) at different externally applied values of the magnetic field, as indicated. Alternating blue, red, and olive lines (color scheme maintained in subsequent panels) represent interpolations of $C_{exp}(T)$ data points (black symbols), while black lines indicate fits of C_Δ given by Eq. (3) to $C_{exp}(T)$ made up to a temperature T_{max}, beyond which an exponential form no longer fits the data. To show the degree of departure, the fitted lines are extrapolated beyond T_{max}. **b** A comparison of Δ values (pink squares) obtained from fits of C_Δ to $C_{exp}(T)$ at different magnetic fields with Δ values (blue circles) obtained by setting $\Delta U = 0$ in Eq. (13). The black dashed line represents $\Delta(B) = \Delta(B = 0) - [g^*_{eff}\sigma]\mu_B B$, which is the expected behavior should Δ be reduced in a magnetic field by Zeeman splitting with $g^*_{eff} = 2.6$ and $\Delta(B=0) = 84$ K. The inset shows n_f values (open pink squares) obtained from fits of C_Δ to $C_{exp}(T)$ in (**a**). All error bars refer to the standard error of the mean.

One possibility is that $\Delta = 84$ K (at $B = 0$) remains constant up to the transition temperature, giving rise to a weakly first-order phase transition (see Fig. 7b) in which the latent heat is similarly small to that depicted in Fig. 7d. In this case, the latent heat must approximately equate to the difference in heat capacity via

$$\Delta U(T) \approx \int (C_{exp} - C_\Delta)\mathrm{d}T \tag{12}$$

in Fig. 4. On considering this as a possibility, we estimate $\Delta U \approx 4$ Jmol^{-1}. This value is somewhat smaller than the value $\Delta U \approx 8$ Jmol^{-1} (shown as a pink square in Fig. 9) obtained from

$$\Delta U(T = T_o) = T_o(S_{exp} - S_\Delta), \tag{13}$$

in which we equate the experimental entropy $S_{exp} \approx 0.2R\ln 2$ associated with excitations at the transition[4,5] (see Methods) with that S_Δ obtained on inserting the fitted values of n_f and $\Delta = 84$ K into Eq. (5). The difference between these estimates suggests that the ~3 K range in temperature over which C_{exp} deviates from C_Δ is too large to be solely attributable to the latent heat of a first-order
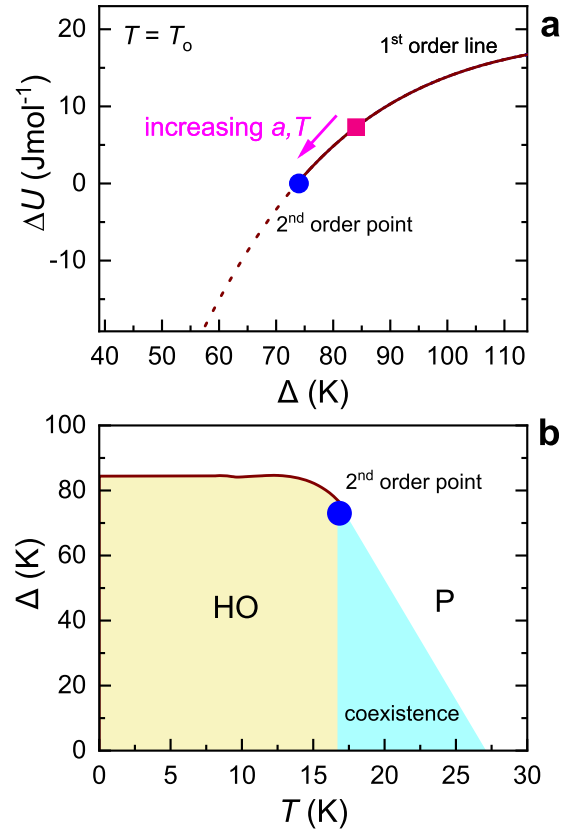

Fig. 9 Vanishing latent heat. a Change in latent heat ΔU of the phase transition between the paramagnetic and hidden-order phases as a function of Δ according to Eq. (13), determined by setting $F_{HO} = F_P$. For large Δ, a finite latent heat causes the transition to be of first order (brown solid line). This is the case for the value of $\Delta = 84$ K (solid pink square) obtained from an Arrhenius plot made for the regime $T \ll T_o$ in Fig. 4. However, at a smaller value of $\Delta \approx 73$ K, ΔU vanishes causing the transition to become of second order (filled blue circle). At smaller values of Δ, the free energies can no longer be made to intersect at $T = T_o$ (dotted brown line). **b** A comparison of the temperature-dependent $\Delta(T)$ (brown line) estimated for $B = 0$ using Eq. (14) and the value of Δ (blue circle) consistent with the second-order end point, identified by setting $\Delta U = 0$ in Eq. (13). Yellow shading indicates where the hidden-order phase exists. Cyan shading illustrates schematically the possible region where phase coexistence due to inhomogeneities of fluctuations is observed.

phase transition. Figure 10a (details provided in the Methods) shows that the difference between $\Delta U(T)$ given by Eq. (12) and ΔU $(T = T_o)$ and given by Eq. (13) occurs for all values of the applied magnetic field.

An alternative possibility is that $\Delta(T)$ undergoes a small reduction on the approach to the transition, leading to an increase in the entropy (and number) of the quasiparticles excited across the gap, and to a further reduction in the value of ΔU given by Eq. (13). On considering such a possibility, Figure 9a shows that there is a narrow range of Δ values for which ΔU is finite, giving rise to a weakly first-order phase transition. Remarkably, however, we find that there exists a value $\Delta \approx 73$ K for which ΔU vanishes (blue circle in Fig. 9a), causing the Ehrenfest classification of the transition to change from first to second order[69]. This value of Δ therefore corresponds to a second-order critical point at the end of a line of first-order phase transitions.

We can verify whether the deviation of the experimental $C_{exp}(T)$ from C_Δ is consistent with a small reduction in $\Delta(T)$ by
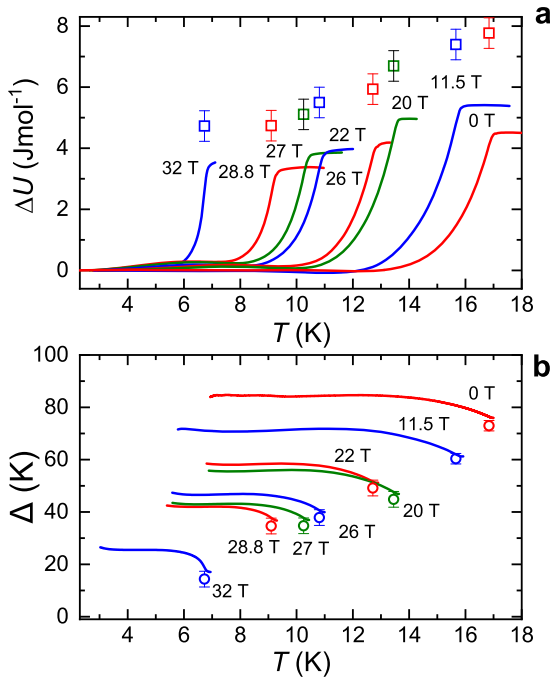
Fig. 10 Comparison of ΔU and Δ estimates. a A comparison of the estimated change in internal energy $\Delta U(T)$ (lines) integrated using Eq. (12), should the transition be of weakly first order, with $\Delta U(T = T_o)$ (open squares) at the transition estimated using Eq. (13). **b** A comparison $\Delta(T)$ (lines) estimated using Eq. (14), should the upturn in C_{exp} be caused by a temperature-dependent gap, with Δ at the transition (open circles) obtained by setting $\Delta U = 0$ in Eq. (13). All error bars refer to the standard error of the mean.

comparing the result (brown line in Fig. 9b) of the integral

$$\Delta(T) \approx \Delta_C - \int_0 \frac{(C_{exp} - C_{\Delta_C})}{n_f R}\left(\frac{T}{\Delta_C}\right)e^{\frac{\Delta_C}{T}}dT \qquad (14)$$

(derived in the Methods, under the assumption that the deviation of C_{exp} from the fitted C_Δ is caused solely by a small reduction in Δ) with the value $\Delta = 73$ K at $T_o(B = 0)$ (blue circle in Fig. 9b) estimated by setting $\Delta U = 0$ in Eq. (13). Consistency between these two estimates at T_o strongly suggests that the HO transition in URu$_2$Si$_2$ lies close to a critical point. We further find that $\Delta(T)$ estimated using Eq. (14) exhibits a similar temperature-dependent change to that obtained in point contact spectroscopy measurements up to T_o[32,33].

On repeating the above analysis at different values of the applied magnetic field (see Fig. 10b and Methods) in Fig. 8a, we always find the same ≈10 K small difference between the values (pink squares in Fig. 8b) of Δ obtained from fits of C_Δ to the heat capacity tail (see Fig. 8a) and the values (blue circles in Fig. 8b) compatible with a second-order critical point in Eq. (13). Since the blue circles collapse to zero before the pink squares on approaching the critical field B_0 in Fig. 8b, we can now understand why the transition becomes of first order at B_0.

We have therefore identified an intriguing situation where a critical point can be realized in which a discontinuity occurs in Δ that coincides with a vanishing (or nearly vanishing) change in the latent heat, giving rise to an unconventional second-order phase transition. The condition for observing a second-order transition may be further relaxed if the separation in temperature between the points at which ΔU and ΔF vanish is less than the width of the phase transition, or in the presence of inhomogeneities or fluctuations(see Methods)[35]. Our finding of a critical point has the potential to shed light on prior reports of a pseudogap in URu$_2$Si$_2$[34], which has further been argued[35] to account for the

continued observation of a gap in point contact spectroscopy measurements over a range of temperatures above T_o[32,33]. The small difference we find in internal energy between the HO and paramagnetic phase at $T > T_0$ further implies that the amplitude of fluctuations of Δ needed for producing a pseudogap is significantly smaller than that required for a BCS-like gap[35] (see Methods).

DISCUSSION

We return to the crucial question in URu$_2$Si$_2$ of whether a symmetry within the HO phase is broken and whether this is responsible for the observed second-order phase transition. Several observations indicate the second-order phase transition into the HO phase of URu$_2$Si$_2$[4,5] to have an unconventional origin. The ratio of the gap magnitude is several times larger than that in the BCS theory[36–39], while the magnitude of the gap is weakly (if at all) suppressed with increasing temperature. Moreover, the pre-factor of the quasiparticle excitations in the specific heat indicates highly degenerate features in the electronic density of states comprising two electrons per formula unit, which are too large to have arisen from Fermi surface nesting (see Methods)[23,25–28]. The large number of states involved suggests instead that the HO phase primarily concerns an electronically driven phase transition in which a hybridization gap between the conduction and f-electron states develops, as has also been inferred from tunneling and neutron scattering experiments[29–33]. Such a scenario differs from that where the amplitude of a broken symmetry order parameter varies continuously at the transition temperature[36–39].

Evidence for an electronic phase transition that modifies the core occupancy of the 5f-electron states is provided by the phase boundary having an elliptical form, closely resembling that found in valence transition systems[51–53], and by significant anomalies in the lattice[45–48]. Pauli paramagnetic limiting of this phase further implies that the electronic excitations retain their spin and charge quantum numbers throughout the HO phase and across the transition, both in weak and strong magnetic fields. Similarities in the magnitude and anisotropy of the quasiparticle g-factor to that previously observed suggest that these are the same quasiparticles that are responsible for the observed quantum oscillations[54,56] and that undergo pairing to produce a superconducting state at low temperatures[55,56,68].

While the near temperature-independence of the electronic structure prior to a discontinuous phase transition with increasing T and the elliptical form of the phase boundary are characteristic features of a first-order transition of the type seen in valence transition systems[51–53], a first-order phase transition is found to exist only at the high magnetic field extremity of the phase boundary[74], where the transition temperature goes to zero. The single most significant factor that distinguishes URu$_2$Si$_2$ from conventional valence transition systems is a semimetallic low temperature phase hosting a large gap in the electronic density of states. At finite temperatures, the robustness of the hybridization gap with increasing temperature is shown to lead to a situation in which the entropy of the quasiparticle excitations increases exponentially with increasing temperature—the experimental signature of which is an exponential tail in the specific heat that spans a wide range in temperature and continues up to the phase transition temperature[4,5]. We show that, by suppressing the latent heat at the transition, the entropy of these excitations has the effect of driving the otherwise discontinuous transition toward a critical point. The combined results and arguments here point to an almost perfect concealment of a first-order transition—turning it continuous in all experimental observables, a condition that could change the way we understand a broad variety of condensed matter systems where order parameters have yet to be identified or where reported broken symmetries cannot easily be reconciled with the magnitude of the excitation gap[1].

METHODS

Possible indirect evidence for broken translational symmetry

While there may also be a separate gap related to a broken translational symmetry order parameter, this gap does not appear to contribute significantly to the point contact spectroscopy, nor to the excitations in the heat capacity or the spin susceptibility, and therefore appears unlikely to be the main driver of the phase transition at T_o. URu$_2$Si$_2$ is known to become antiferromagnetic with a doubled unit cell under pressure[1,23], giving rise to a possible situation analogous to those in UPd$_2$Al$_3$[75] and U(Pt$_{1-x}$Pd$_x$)$_3$[76] in which hybridized bands (and possibly a hybridization gap) coexist with large moment antiferromagnetism. In URu$_2$Si$_2$, photoemission and quantum oscillation studies have reported evidence for Fermi surface nesting also to exist within the ambient pressure HO phase[23,25–28]. The proposed nesting within the HO phase, however, pertains to small sections of Fermi surface for which the number of gapped states[24] is one or two orders of magnitude smaller than the gapped states we identify to be responsible for the quasiparticle excitations in specific heat measurements. An alternative possibility is that the small Fermi surface pockets are the pre-existing product of a Kondo semimetallic ground state, and that the antiferromagnetism observed under pressure is secondary. The Fermi surface pockets in URu$_2$Si$_2$ are sufficiently small and different in size and small in number, that there is a reasonably large probability for them not to intersect each other upon halving the Brillouin zone, in which case they would be expected to remain largely unchanged on entering the antiferromagnetic phase. Interpretations of quantum oscillations are also constrained by the fact that whereas ambient pressure quantum oscillation experiments can be used to infer the shapes of the Fermi surface pockets, this has not been done under pressure[23].

Specific heat background subtraction

Following the procedure outlined in previously published specific heat measurements[49,57], the phonon contribution is obtained from measurements of ThRu$_2$Si$_2$ (see Fig. 2). After subtracting the phonon component, the remaining heat capacity is assumed to be electronic in origin. At $B = 0$, the exponential contribution to the heat capacity is observed to extend down to ≈6 K, below which the specific heat is observed to have a residual contribution $C(T) \approx \gamma_{HO}T$.

In order to extract the form of C_{exp} attributable to excitations within the HO phase, $\gamma_{HO}T$ needs to be subtracted. This was initially done by subtracting a constant γ_{HO} from the measured C/T[5]. More recent heat capacity studies have shown that γ_{HO} increases slowly with decreasing temperature. Moriya and Takimoto[77] and van Dijk et al.[57] attributed this behavior to spin fluctuations, originating from the close proximity of URu$_2$Si$_2$ to an antiferromagnetic ground state. Throughout the manuscript, we have assumed $\gamma_{HO}(T)$ to have the form determined by van Dijk et al. (see Fig. 2).

Alternatives to a hybridization gap at $T > T_o$

Given the finding of a Fano line shape at $T > T_o$ in scanning tunneling microscopy measurements on URu$_2$Si$_2$[29,30], which is generally considered to be consistent with a lattice of locally screened Kondo impurities, we might expect the electronic contribution to C/T to have the form of a Schotte–Schotte anomaly[78]. A Zeeman-split Schotte–Schotte anomaly has been shown to provide a good approximation to the evolution of C/T over a wide range of magnetic fields in the sister heavy fermion compound CeRu$_2$Si$_2$ and at $B > 40$ T in URu$_2$Si$_2$[79]. The various phase transitions in URu$_2$Si$_2$ prevent us from verifying whether a Schotte–Schotte anomaly describes the paramagnetic phase for $B < 40$ T and $T > T_o$, however. We therefore make the simplifying assumption that $\Delta\gamma$ and $\Delta\chi_{zz}$ are constants in Eq. (6)—an approximation that appears to be valid up to ≈25 K in Fig. 2a.

Free energy contribution Φ_Δ from gap excitations

While the Φ_Δ term gives a prominent contribution to the specific heat $C_\triangle = -T\frac{\partial^2\Phi_\Delta}{\partial T^2}$ within the HO phase, its overall contribution to the free energy is smaller by a factor $(\Delta/T)^2$, making its contribution only a small fraction of U_o. Nevertheless, the question remains as to whether Φ_Δ causes a discernible departure of the phase boundary from the elliptical form. To test this, in Fig. 3b we plot Φ_Δ (using the fitted parameters n_f and Δ in Fig. 8) as a function of the reduced temperature $T/T_o(B)$, finding it to reach a similar value $\Phi \approx 1.5 \pm 0.1$ Jmol^{-1} at the phase boundary at nearly all values of the magnetic field. The largest deviation occurs for the highest magnetic field datapoint at 32 T, but the fact that no corresponding deviation is observed in Fig. 5 suggests that the deviation in Fig. 3b points to the

source of the error originating from the fitting of C_Δ over a short range of T at the highest magnetic field. The differences in the values of Φ_Δ at the transition appear to be too small to cause a significant departure of the phase diagram from the elliptical form.

Departures of C_Δ from C_{exp} approaching T_o

While the accuracy of fitting C_Δ in Fig. 8 is likely to be reduced in strong magnetic fields due to a reduction in the temperature range, the degree of departure of the experimental specific heat C_{exp} from a simple exponential form becomes significantly more pronounced. We consider two possible sources of the departure of C_{exp} from C_Δ.

Latent heat change at a weakly first order transition: in the case of a first-order phase transition, a fit of C_Δ given by Eq. (3) to the specific heat data in Figs. 2 and 8a is expected to apply everywhere, except very close to the transition where the latent heat ΔU causes an upturn in the heat capacity. There, we expect an integration of the heat capacity minus the fit to yield a change in internal energy ($\Delta U(T)$ in Eq. (12)) that is the same as the difference in internal energy between the phases given by Eq. (13). We verify this not to be the case in Fig. 10a.

Change in Δ near a second-order phase transition: the alternative possibility is that ΔU is tuned to zero near the transition, causing the Ehrenfest classification of the transition to become of second order. One way this can happen is if $\Delta(T)$ falls with increasing temperature as is, for example, reported to occur in point contact spectroscopy measurements[32]. Since the strength of hybridization is generally weakened as the lattice spacing a between f-electron sites increases, the increase in the lattice parameter a accompanying the transition into the high temperature paramagnetic phase could be one possible factor in causing the transition to become of second order. In this case, we would expect the reduction in $\Delta(T)$ with increasing T to be responsible for the upturn in the specific heat close to the transition temperature.

To estimate the effect of a temperature-dependent gap $\Delta(T)$ on C, we reduce Eq. (2) to a more approximate form

$$\Phi_0 \approx -n_f RT e^{-\frac{\Delta(T)}{T}}$$

(given that $e^{-\frac{\Delta(T)}{T}} \ll 1$), from which we obtain

$$C \approx n_f R e^{-\frac{\Delta}{T}}\left(1 + \left(\frac{\Delta^2}{T^2} + \frac{\partial\Delta}{\partial T}\left(1 - \frac{\Delta}{T}\right)\right. \right.$$
$$\left.\left. -T\frac{\partial^2\Delta}{\partial T^2} + \left(\frac{\partial\Delta}{\partial T}\right)^2\right)\right) \tag{15}$$

after double differentiation. Assuming the limits $\Delta/T \gg 1$ and $\Delta/T \gtrsim \partial\Delta/\partial T$, we obtain the approximate result

$$C \approx C_\Delta - n_f RT e^{-\frac{\Delta}{T}}\left(\frac{\Delta}{T}\frac{\partial\Delta}{\partial T}\right), \tag{16}$$

which we rearrange to yield Eq. (14), from which $\Delta(T)$ can be estimated numerically (lines in Fig. 10b).

Meanwhile, the smallest permissible equilibrium value of Δ is that corresponding to an end point in Fig. 9a. We determine this value by setting $\Delta U = 0$ in Eq. (13)—yielding an equation

$$S_\Delta(\Delta, T_o) = S_{exp} \tag{17}$$

that can be solved for $\Delta(T_o(B))$, the results of which are plotted in Fig. 10b (circles). Here, $T_o(B)$ refers to the value of the transition temperature in a magnetic field. Consistency between the value of $\Delta(T)$ at $T_o(B)$ (i.e., the highest temperature limit of the lines in Fig. 10b) estimated using Eqs. (16) and (14) and that obtained independently for a second-order end point by solving Eq. (17) suggests that $\Delta(T)$ retains a near constant value until close to the transition, but then ultimately falls by ≈10 K to produce a second-order end point. For smaller values of Δ, the free energy curves (e.g., that in Fig. 7b) given by Eq. (6) cannot be made to intersect at $T = T_o(B)$. Only fluctuations of Δ are therefore possible once $T > T_o(B)$, and their existence is strongly suggested by the near-degeneracy in the free energy curves in this regime. This is also the same regime in which a pseudogap or crossover is observed in spectroscopic experiments[32–34,59].

Changes in internal energy

In the case of a BCS order parameter, we would expect $U_o = \frac{1}{2}D(\varepsilon)(k_B\Delta)^2 \approx \frac{3}{2\pi^2}\Delta\gamma\Delta^2$ (noting that Δ is expressed in degrees kelvin), from which we estimate $U_o \approx 73$ Jmol^{-1}. The fact that this is much larger than the actual value of $U_o \approx 8$ Jmol^{-1} in Fig. 7b again reinforces our prior finding that the observed gap does not originate solely from states at the Fermi surface. An alternative scenario in the case of a hybridization

transition is that U_o is the consequence of a difference in energy between competing electronic configurations (possibly with different numbers of $5f$ electrons confined to the atomic core), and $\Delta = 84$ K is determined independently by V. If Δ does at some point change, then one would expect the dependence of U_o on Δ to be parabolic to lowest order, so that $U_o = U_{o,0} - U'(\Delta - \Delta_0)^2$, where $U' \ll \frac{3}{2\pi^2}\Delta\gamma$ and $U_{o,0}$ is the low temperature value valid for $\Delta = \Delta_0$; here, Δ_0 refers specifically to the value of Δ determined from lower temperature fits in Fig. 4.

Fluctuations and pseudogap formation

Owing to the likely discontinuous nature of the change in Δ, an interesting situation arises in which fluctuations can cause phase coexistence to occur at a second-order phase transition. One possible source of fluctuations or inhomogeneities is the proximity to the antiferromagnetically ordered phase under pressure[35], which has already been shown to give rise to a tiny volume fraction of antiferromagnetic order within the HO phase[1]. Indeed, one of the more unusual discoveries in recent spectroscopy experiments[32–34,59] in URu_2Si_2 is the emergence of what appears to be a coexistence region, pseudogap, or crossover at temperatures $T > T_o$, which also has the unusual property (depending on the experimental technique) of the gap maintaining a finite amplitude on passing through $T = T_o$, despite the phase transition. The discontinuous change in Δ that we have identified implies that fluctuations can give rise to regions with a full gap amplitude ($73 \leq \Delta \leq 84$ K) coexisting with regions with an absent hybridization gap in the paramagnetic state (see Methods). Such a scenario is made likely by the very small difference in free energy between the fully gapped HO state and the paramagnetic state (see Fig. 7b) over a range of temperatures $T > T_o$. The normal state maximum at ~22 K in Fig. 2a is indeed consistent with a heavily broadened gap of ~73 K.

By considering a BCS-like order parameter, Haraldsen et al.[35] were able to simulate a pseudogap, but with the caveat that the amplitude σ_Δ of the order parameter fluctuations was required to be $\approx 60\%$ of Δ, bringing into question the viability of a sharp phase transition in URu_2Si_2. In the present work, the extreme sensitivity of the transition to small changes in Δ means that a pseudogap over a substantial region of T can be realized with fluctuations that are only a small fraction of Δ. Gap fluctuations of amplitude σ_Δ produce a statistical broadening of the HO free energy of size

$$\sigma_{\Delta F} \approx \sigma_\Delta \times \left|\frac{\partial \Phi_\Delta}{\partial \Delta}\right| \approx n_f R \sigma_\Delta \frac{e^{-\frac{\Delta}{T}}}{1 + e^{-\frac{\Delta}{T}}}. \tag{18}$$

We find that $\sigma_\Delta/\Delta = 5\%$ is all that is required for $\sigma_{\Delta F}$ to become comparable to the ≈ 0.5 Jmol^{-1} difference in free energy between the curves at $T \sim 20$ K in Fig. 7b.

Given the lattice changes at the transition, fluctuations would further be expected to affect the lattice dynamics of URu_2Si_2. Thermal expansion measurements have previously shown that the HO and paramagnetic phases have different values of the c/a ratio (the ratio of the c-axis to the a-axis lattice parameters)[45,46,48], implying that this ratio is coupled to the strength of the hybridization and Δ. Fluctuations of Δ within the pseudogap region are therefore likely to lead to a considerable softening of the crystalline lattice with respect to the A_{1g} mode. A lattice softening of this nature has recently been reported in resonant ultrasound spectroscopy experiments[80], although the existing interpretation has assumed strictly localized $5f$ electrons—in effect, neglecting the extreme sensitivity of the f-electron core occupancy and hybridization strength to volume changes and lattice distortions. Because it preserves the fourfold symmetry of the lattice, the A_{1g} mode is the only one (other than a change in volume) that couples to the degree of delocalization of the $5f$ electrons (and thereby the strength of Δ) uniformly across all sites.

DATA AVAILABILITY

The datasets generated during and/or analyzed during the current study are available from the corresponding author on reasonable request.

REFERENCES

1. Mydosh, J. A. & Oppeneer, P. M. Hidden order, superconductivity, and magnetism: the unsolved case of URu_2Si_2. Rev. Mod. Phys. **83**, 1301–1322 (2011).
2. Kasuya, T. Hidden ordering and heavy mass in URu_2Si_2 and its alloys. J. Phys. Soc. Jpn. **66**, 3348–3351 (1997).
3. Chandra, P., Coleman, P., Mydosh, J. A. & Tripathi, V. Hidden orbital order in the heavy fermion metal URu_2Si_2. Nature **417**, 831–834 (2002).
4. Palstra, T. T. M. et al. Superconducting and magnetic transitions in the heavy-fermion system URu_2Si_2. Phys. Rev. Lett. **55**, 2727–2730 (1985).
5. Maple, M. B. et al. Partially-gapped Fermi-surface in the heavy-electron superconductor URu_2Si_2. Phys. Rev. Lett. **56**, 185–188 (1986).
6. Varma, C. M. & Zhu, L. J. Helicity order: hidden order parameter in URu_2Si_2. Phys. Rev. Lett. **96**, 036405 (2006).
7. Okazaki, R. et al. Rotational symmetry-breaking in the hidden-order phase of URu_2Si_2. Science **331**, 439–442 (2011).
8. Santini, P. & Amoretti, G. Crystal-field model of the magnetic-properties of URu_2Si_2. Phys. Rev. Lett. **73**, 1027–1030 (1994).
9. Barzykin, V. & Gorakov, L. P. Singlet magnetism in heavy fermions. Phys. Rev. Lett. **74**, 4301–4304 (1995).
10. Ikeda, H. & Ohashi, Y. Theory of unconventional spin density wave: a possible mechanism of the micromagnetism in U-based heavy fermion compounds. Phys. Rev. Lett. **81**, 3723–3726 (1998).
11. Ohkawa, F. J. & Shimizu, H. Quadrupole and dipole orders in URu_2Si_2. J. Phys. Condens. Matter **11**, L519–L524 (1999).
12. Kiss, A. & Fazekas, P. Group theory and octupolar order in URu_2Si_2. Phys. Rev. B **71**, 054415 (2005).
13. Haule, K. & Kotliar, G. Arrested Kondo effect and hidden order in URu_2Si_2. Nat. Phys. **5**, 796–799 (2009).
14. Elgazzar, S. et al. Hidden order in URu_2Si_2 originates from Fermi surface gapping induced by dynamic symmetry-breaking. Nat. Mater. **8**, 337–341 (2009).
15. Harima, H., Miyake, K. & Flouquet, J. Why the hidden order in URu_2Si_2 Is still hidden—one simple answer. J. Phys. Soc. Jpn. **79**, 033705 (2010).
16. Kusunose, H. & Harima, H. On the hidden order in URu_2Si_2 - antiferro hexadecapole order and its consequences. J. Phys. Soc. Jpn. **80**, 084702 (2011).
17. Fujimoto, S. Spin nematic state as a candidate of the hidden order phase of URu_2Si_2. Phys. Rev. Lett. **106**, 196497 (2011).
18. Pepin, C., Norman, M. R., Burdin, S. & Ferraz, A. Modulated spin liquid: a new paradigm for URu_2Si_2. Phys. Rev. Lett. **106**, 106601 (2011).
19. Dubi, Y. & Balatsky, A. V. Hybridization wave as the "hidden order" in URu_2Si_2. Phys. Rev. Lett. **106**, 086401 (2011).
20. Ikeda, H. et al. Emergent rank-5 nematic order in URu_2Si_2. Nat. Phys. **8**, 528–533 (2012).
21. Chandra, P., Coleman, P. & Flint, R. Hastatic order in the heavy-fermion compound URu_2Si_2. Nature **493**, 621–626 (2013).
22. Kung, H. H. et al. Chirality density wave of the "hidden order" phase in URu_2Si_2. Science **347**, 1339–1342 (2015).
23. Hassinger, E. et al. Similarity of the Fermi surface in the hidden order state and in the antiferromagnetic state of URu_2Si_2. Phys. Rev. Lett. **105**, 216409 (2010).
24. Oppeneer, P. M. et al. Electronic structure theory of the hidden-order material URu_2Si_2. Phys. Rev. B **82**, 205103 (2010).
25. Santander-Syro, A. F. et al. Fermi-surface instability at the 'hidden-order' transition of URu_2Si_2. Nat. Phys. **5**, 637–641 (2009).
26. Meng, J.-Q. et al. Imaging the three-dimensional Fermi-surface pairing near the hidden-order transition in URu_2Si_2 using angle-resolved photoemission spectroscopy. Phys. Rev. Lett. **111**, 127002 (2013).
27. Yoshida, R. et al. Translational symmetry breaking and gapping of heavy-quasiparticle pocket in URu_2Si_2. Sci. Rep. **3**, 2750 (2013).
28. Bareille, C. et al. Momentum-resolved hidden-order gap reveals symmetry breaking and origin of entropy loss in URu_2Si_2. Nat. Commun. **5**, 4326 (2014).
29. Schmidt, A. R. et al. Imaging the Fano lattice to 'hidden order' transition in URu_2Si_2. Nature **465**, 570–576 (2010).
30. Aynajian, P. et al. Visualizing the formation of the Kondo lattice and the hidden order in URu_2Si_2. Proc. Natl Acad. Sci. USA **107**, 10383–10388 (2010).
31. Butch, N. P. et al. Symmetry and correlations underlying hidden order in URu_2Si_2. Phys. Rev. B **91**, 035128 (2015).
32. Park, W. K. et al. Observation of the hybridization gap and Fano resonance in the Kondo lattice URu_2Si_2. Phys. Rev. Lett. **108**, 246403 (2012).
33. Hasselbach, K., Kirtley, J. R. & Lejay, P. Point-contact spectroscopy of superconducting URu_2Si_2. Phys. Rev. B **46**, 5826–5829 (1992).
34. Liu, M. K. et al. Evidence of a hidden-order pseudogap state in URu_2Si_2 using ultrafast optical spectroscopy. Phys. Rev. B **84**, 161101 (2011).
35. Haraldsen, J. T., Dubi, Y., Curro, N. J. & Balatsky, A. V. Hidden-order pseudogap in URu_2Si_2. Phys. Rev. B **84**, 214410 (2011).
36. Bardeen, J., Cooper, I. N. & Schrieffer, J. R. Theory of superconductivity. Phys. Rev. **108**, 1175–1204 (1957).
37. Grüner, G. Density waves in solids (Addison-Wesley, 1994).
38. Tinkham, M. Introduction to superconductivity (McGraw-Hill, Inc., New York, 1996).

39. Johnston, D. C. Elaboration of the α-model derived from the BCS theory of superconductivity. *Supercond. Sci. Technol.* **26**, 115011 (2013).

40. Hewson, A. C. *The Kondo problem to heavy fermions* (Cambridge University Press, Cambridge, 1993).

41. Coleman, P. *Introduction to many-body physics* (Cambridge University Press, Cambridge, 2015).

42. Lawrence, J. W., Riseborough, P. S. & Parks, R. D. Valence fluctuation phenomena. *Rep. Prog. Phys.* **44**, 1–84 (1981).

43. Jeffries, J. R., Moore, K. T., Butch, N. P. & Maple, M. B. Degree of $5f$ electron localization in $URu_2 Si_2$: electron energy-loss spectroscopy and spin-orbit sum rule analysis. *Phys. Rev. B* **82**, 033103 (2010).

44. Booth, C. H. et al. Probing $5f$-state configurations in $URu_2 Si_2$ with U L_{111}-edge resonant x-ray emission spectroscopy. *Phys. Rev. B* **94**, 045121 (2016).

45. de Visser, A., Kayzel, F. E., Menovsky, A. A. & Franse, J. J. M. Thermal expansion and specific heat of monocrystalline $URu_2 Si_2$. *Phys. Rev. B* **34**, 8168–8171 (1986).

46. Motoyama, G., Nishioka, T. & Sato, N. K. Phase transition between hidden and antiferromagnetic Order in $URu_2 Si_2$. *Phys. Rev. Lett.* **90**, 166402 (2003).

47. Correa, V. F. et al. High-magnetic-field lattice length changes in $URu_2 Si_2$. *Phys. Rev. Lett.* **109**, 246405 (2012).

48. Wartenbe, M. et al. Magnetoelastic coupling in $URu_2 Si_2$: probing multipolar correlations in the hidden order state. *Phys. Rev. B* **99**, 235101 (2019).

49. Jaime, M. et al. High magnetic field studies of the hidden order transition in $URu_2 Si_2$. *Phys. Rev. Lett.* **89**, 287201 (2002).

50. Kim, J. S., Hall, D., Kumar, P. & Stewart, G. R. Specific heat of $URu_2 Si_2$ in fields up to 42 T: clues to the hidden order. *Phys. Rev. B* **67**, 014404 (2003).

51. Dzero, M. O., Gor'kov, L. P. & Zvezdin, A. K. First-order valence transition in $YbInCu_4$ in the (B, T)-plane. *J. Phys. Condens. Matter* **12**, L711–L718 (2000).

52. Immer, C. D., Sarrao, J. L. & Fisk, Z. Magnetic-field, pressure, and temperature scaling of the first-order valence transition in pure and doped $YbInCu_4$. *Phys. Rev. B* **56**, 71–74 (1997).

53. Drymiotis, F. et al. Suppression of the γ-α structural phase transition in $Ce_{0.8} La_{0.1} Th_{0.1}$ by large magnetic fields. *J. Phys. Condens. Matter* **17**, L77–L83 (2005).

54. Altarawneh, M. M. et al. Sequential spin polarization of the Fermi surface pockets in $URu_2 Si_2$ and Its Implications for the hidden order. *Phys. Rev. Lett.* **106**, 146403 (2011).

55. Altarawneh, M. M. et al. Superconducting pairs with extreme uniaxial anisotropy in $URu_2 Si_2$. *Phys. Rev. Lett.* **108**, 066407 (2012).

56. Bastien, G. et al. Fermi-surface selective determination of the g-factor anisotropy in $URu_2 Si_2$. *Phys. Rev. B* **99**, 165138 (2019).

57. van Dijk, N. H. et al. Specific heat of heavy-fermion URu_2Si_2 in high magnetic fields. *Phys. Rev. B* **56**, 14493–14498 (1997).

58. Lee, P. A., Rice, T. M. & Anderson, P. W. Fluctuation effects at a Peierls transition. *Phys. Rev. Lett.* **31**, 462–465 (1973).

59. Levallois, J. et al. Hybridization gap and anisotropic far-infrared optical conductivity of $URu_2 Si_2$. *Phys. Rev. B* **84**, 184420 (2011).

60. Bachar, N. et al. Detailed optical spectroscopy of hybridization gap and hidden-order transition in high-quality $URu_2 Si_2$ single crystals. *Phys. Rev. B* **94**, 235101 (2016).

61. Schoenes, J., Schönenberger, Franse, J. J. M. & Menovsky, A. A. Hall-effect and resistivity study of the heavy-fermion system $URu_2 Si_2$. *Phys. Rev. B* **35**, 5375–5378 (1987).

62. Nagel, U. et al. Optical spectroscopy shows that the normal state of $URu_2 Si_2$ is an anomalous Fermi liquid. *Proc. Natl Acad. Sci. USA* **109**, 19161–19165 (2012).

63. López de la Torre, M. A. et al. Low temperature specific heat of $URu_2 Si_2$ near the superconducting transition. *Phys. B* **165–166**, 385–386 (1990).

64. Harrison, N., Jaime, M. & Mydosh, J. A. Reentrant hidden order at a metamagnetic quantum critical end point. *Phys. Rev. Lett.* **90**, 096402 (2003).

65. Bergemann, C. et al. Quantum oscillations in $URu_2 Si_2$. *Physica B* 348–350 (1997).

66. Ohkuni, H. et al. Fermi surface properties and de Haas-van Alphen oscillation in both the normal and superconducting mixed states of $URu_2 Si_2$. *Philos. Mag. B* **79**, 1045–1077 (1999).

67. Trinh, J. et al. Thermodynamic measurement of angular anisotropy at the hidden order transition of $URu_2 Si_2$. *Phys. Rev. Lett.* **117**, 157201 (2016).

68. Hattori, T. et al. Evidence for spin singlet pairing with strong uniaxial anisotropy in $URu_2 Si_2$ using nuclear magnetic resonance. *Phys. Rev. Lett.* **120**, 027001 (2018).

69. Jaeger, G. The Ehrenfest classification of phase transitions: introduction and evolution. *Arch. Hist. Exact. Sci.* **53**, 51–81 (1998).

70. Ashcroft, N. W. & Mermin, N. D. *Solid state physics* (Saunders College Publishing, Orlando, 1976).

71. Jo, Y. J. et al. Field-induced Fermi surface reconstruction and adiabatic continuity between antiferromagnetism and the hidden-order state in $URu_2 Si_2$. *Phys. Rev. Lett.* **98**, 166404 (2007).

72. Clogston, A. M. Upper limit for the critical field in hard superconductors. *Phys. Rev. Lett.* **9**, 266–267 (1962).

73. Chandrasekhar, B. S. A note on the maximum critical field of high-field superconductors. *Appl. Phys. Lett.* **1**, 7–8 (1962).

74. Kim, K. H. et al. Magnetic-field-induced quantum critical point and competing order parameters in $URu_2 Si_2$. *Phys. Rev. Lett.* **91**, 256401 (2003).

75. Haga, Y. et al. De Haas-van Alphen oscillation in both the normal and superconducting mixed states of $UPd_2 Al_3$. *J. Phys. Soc. Jpn.* **68**, 342–345 (1999).

76. Graf, M. J. et al. Onset of antiferromagnetism in UPt_3 via Th substitution studied by muon spin spectroscopy. *Phys. Rev. B* **88**, 224421 (2003).

77. Moriya, T. & Takimoto, T. Anomalous properties around magnetic instability in heavy electron systems. *J. Phys. Soc. Jpn.* **64**, 960–969 (1994).

78. Schotte, K. D. & Schotte, U. Interpretation of Kondo experiments in a magnetic field. *Phys. Lett. A* **55A**, 38–40 (1975).

79. Silhanek, A. V. et al. Quantum critical $5f$ electrons avoid singularities in $URu_2 Si_2$. *Phys. Rev. Lett.* **95**, 026403 (2005).

80. Ghosh, S. et al. One-component order parameter in $URu_2 Si_2$ uncovered by resonant ultrasound spectroscopy and machine learning. *Prepring. Sci. Adv.* **6**, eaaz4074 (2020).

ACKNOWLEDGEMENTS

AUTHOR CONTRIBUTIONS

Measurements were performed by M.J., S.K.K., M.K.C., and N.H.; the analysis was performed by N.H.; and the paper was written by N.H. and M.J.

COMPETING INTERESTS

The authors declare no competing interests.

ADDITIONAL INFORMATION

Correspondence and requests for materials should be addressed to N.H.

Reprints and permission information is available at http://www.nature.com/reprints

Publisher's note Springer Nature remains neutral with regard to jurisdictional claims in published maps and institutional affiliations.